ELSEVIER

Journal of Electroanalytical Chemistry 500 (2001) 279–289

Journal of Electroanalytical Chemistry

www.elsevier.nl/locate/jelechem

Scanning electrochemical microscopy of hydrogen electro-oxidation. Rate constant measurements and carbon monoxide poisoning on platinum

Krishnakumar Jambunathan, Biren C. Shah, John L. Hudson, Andrew C. Hillier *

Department of Chemical Engineering and Center for Electrochemical Science and Engineering, University of Virginia, Charlottesville, VA 22903-2442, USA

Received 13 June 2000; received in revised form 11 August 2000; accepted 14 August 2000

Dedicated to Professor R. Parsons on the occasion of his retirement from the position of the Editor in Chief of the Journal of Electroanalytical Chemistry and in recognition of many contributions to electrochemistry

Abstract

We describe an application of the scanning electrochemical microscope that uses tip–sample feedback to characterize the electro-oxidation of hydrogen on a polycrystalline platinum electrode in sulfuric acid solutions in the presence and absence of adsorbed carbon monoxide. The hydrogen oxidation reaction is probed by reducing protons at a diffusion-limited rate at the microscope's tip electrode while it is positioned near a platinum substrate. A series of approach curves measured as a function of the substrate potential provides hydrogen oxidation rate constant values over a wide range of substrate conditions. In the absence of CO, the rate of hydrogen oxidation exceeds 1 cm s^{-1} at potentials within the hydrogen adsorption and double layer charging regions. A Tafel slope of ~ 30 mV per decade is determined near the reversible potential. At increasingly positive substrate potentials, the hydrogen oxidation rate decreases exponentially with increasing potential as the surface is covered with an oxide layer. The adsorption of solution-phase carbon monoxide completely deactivates the platinum substrate towards steady-state hydrogen oxidation over a large range of substrate potentials. Approach curves indicate a near-zero rate constant for hydrogen oxidation on CO-covered platinum at potentials below oxide formation. An increase in the hydrogen oxidation rate is seen at potentials sufficiently positive that CO fails to adsorb and the platinum oxide forms. In comparison, dynamic tip–substrate voltammetry depicts a complex substrate response whereby the adsorbed carbon monoxide layer transforms from a weakly adsorbed state at low potentials to a strongly adsorbed state at high potentials. Although steady-state approach curve measurements depict the complete deactivation of catalytic activity at these potentials, a significant hydrogen oxidation current is observed during the potential-induced transformation between these weakly and strongly adsorbed CO states. The rate of hydrogen oxidation approaches that of a pristine platinum surface during this surface transformation before returning to the poisoned state.

Keywords: Scanning electrochemical microscopy; Microelectrode; Electrocatalysis; Carbon monoxide; Hydrogen oxidation; Platinum; Fuel cell

1. Introduction

The hydrogen oxidation reaction is of fundamental scientific importance as a model electrocatalytic reaction and has significant practical utility as a popular anode reaction in fuel cells. Hydrogen oxidation has been the subject of exhaustive examination in order to understand the kinetics, mechanism and characteristics of this reaction on a variety of metal electrodes in numerous electrolyte systems [1–7]. Recently, a resurgence of interest in hydrogen oxidation has emerged as fuel cells have regained popularity. In addition, our understanding of the hydrogen oxidation reaction has improved as our ability to prepare well defined single crystals and multi-component catalyst electrodes has developed along with our ability to characterize and evaluate accurately the electrode | electrolyte interface. A variety of traditional electrochemical techniques as

* Corresponding author. Tel.: +1-804-924-1302; fax: +1-804-982-2658.

E-mail address: ach3p@virginia.edu (A.C. Hillier).

0022-0728/01/$ - see front matter
PII: S0022-0728(00)00344-2

well as more novel surface science and analytical methods have been applied to this system. Hydrogen oxidation has been extensively studied on pure and multicomponent metal catalysts in order to develop an understanding of the reactivity of various catalyst materials [8], to deduce the influence of surface structure and crystal orientation on reactivity [4,7,9], and to elucidate the role of various electrode-deactivating poisons [10–12] and activity enhancing species on this reaction.

Catalyst poisoning through the adsorption of electrode deactivating species is of significant practical consequence. In particular, fuel cell anodes that utilize hydrocarbon-based fuels are limited in their ability to actively catalyze oxidation reactions in the presence of electrode deactivating adsorbates that appear as reaction intermediates or as fuel by-products. An example of the former would be the deactivation of platinum during methanol oxidation via a reaction intermediate and the latter occurs for fuels based upon industrial hydrogen or hydrogen generated from hydrocarbon reforming. Catalyst deactivation in electrochemical systems has been the subject of intense study in order to understand better the nature of the adlayers and to develop alternative catalysts with greater poison tolerance [10,12–17]. Our knowledge of CO-adlayers has improved considerably with the use of in-situ FTIR [18] [19–21], sum frequency generation [22], mass spectrometry [14], scanning tunneling microscopy [23,24], and careful electrochemical measurements. The mechanism of CO adsorption, oxidation and its influence on hydrogen oxidation have been extensively studied and several highly promising CO-tolerant anode materials have been discovered based upon platinum alloys with Ru [25–30], Sn [31,32] and Mo [33–35].

Much of the electrochemical data on hydrogen oxidation kinetics and CO deactivation has been acquired using hydrodynamic methods, such as the rotating disk electrode (RDE). However, mechanical limitations and the onset of fluid turbulence limit the ability of RDE techniques to access extremely high rate constants. Notably, the high mass transfer rates achievable at microelectrodes have allowed access to kinetic regimes in excess of those typically obtainable with RDE techniques [36]. In fact, the combination of a microelectrode and capillary jet has been shown to produce mass transfer characteristics equivalent to a RDE rotating at 200 000 Hz [37]. Alternatively, the ability of a scanning electrochemical microscope (SECM) to position a microelectrode probe near a substrate | electrolyte interface creates mass transfer between tip and sample (proportional to their separation) that is sufficiently high to allow access to kinetic rate constants two to three orders of magnitude higher than that allowed with RDE [38]. The tip response can also be used to decouple substrate processes by measuring a specific reaction. This capability exceeds that of rotating ring-disk configurations because the separation between tip and sample can be adjusted independently to vary the detection mechanism from one that samples reaction kinetics (feedback mode) to one that is used for analyte detection or substrate dosing (generator-collector mode). In addition, the ability to perform interfacial measurements as a function of spatial position allows the SECM to perform direct structure–function measurements on catalytic surfaces by imaging variations in reactivity with changes in surface composition or structure. We have recently described how catalytic activity can be characterized over heterogeneous surfaces to deduce the local reactivity due to changes in substrate composition [39].

In this paper we describe an application of the scanning electrochemical microscope (SECM) that utilizes tip–sample feedback to characterize the hydrogen oxidation reaction on a polycrystalline platinum surface. The kinetics of hydrogen oxidation are examined on platinum over a large range of substrate potentials from the hydrogen adsorption region to deep into the platinum oxide region. Approach curve and tip–substrate voltammetry measurements are used to determine the rate constant for hydrogen oxidation using standard curve-fitting procedures. The influence of adsorbed CO is also explored. SECM measurements are used to characterize both the steady state poisoning of platinum by CO as well as the complexity of the adsorbed CO and its influence on the hydrogen oxidation reaction.

2. Experimental

2.1. Materials

All experiments were performed using electrolytes dissolved in 18 MΩ deionized water (Milli-Q, Millipore Corp., Bedford, WA). For CO-free experiments, the solutions were de-aerated with argon (BOC Gases, Murray Hill, NJ) prior to measurement. Electrolyte solutions included sulfuric acid (H_2SO_4) and sodium sulfate (Na_2SO_4) (Aldrich, Milwaukee, WI), which were used as received. In carbon monoxide poisoning experiments, CO (BOC Gases, Murray Hill, NJ) was delivered to the electrochemical apparatus by bubbling the gas through a porous ceramic frit (Ace Glass) for 5–15 min prior to measurement.

2.2. Scanning electrochemical microscope

The scanning electrochemical microscope (SECM) used in this work was similar to that described in the literature [40–43]. Three inchworm translation motors (model IW-710, Burleigh Instruments, Inc., Fishers, NY) were mounted directly onto one TS-300 (z) and two TS-100 (xy) translation stages configured for three-

dimensional orthogonal motion. These stages were mounted directly to a vibration isolation platform and the entire assembly was enclosed in a Faraday cage. The inchworm motors had a 25 mm range of motion, a mechanical resolution of 4 nm and optical encoders giving an absolute position reproducibility of 0.5 μm. Position control was achieved with a series 7000 controller (Burleigh Instruments, Inc., Fishers, NY) interfaced to a GPIB-PCIIA IEEE-488 interface card (National Instruments, Austin, TX). Electrochemical measurements were performed using a bipotentiostat (model AFDRE, PINE Instrument Company, Grove City, PA) coupled with a high sensitivity current amplifier (Keithley Instruments, Inc., Cleveland, OH), which was used to measure the current at the microelectrode tip. Data collection and tip scanning were achieved with a multi-channel data acquisition board (PCL818, Advantek, Minnetonka, MN) and a custom software program written in Visual Basic™.

The electrochemical cell for SECM experiments was made from Teflon with a cell volume of 15 ml. The cell contained slots for reference, counter and substrate electrodes. The substrate electrode was positioned in a slot at the bottom of the cell with a vertical orientation and the electrode surface facing upwards. The cell was made leak-proof by pressure fitting all electrodes with Teflon tape.

2.3. Electrodes

The microelectrode tips employed in the SECM were fabricated with 25 μm diameter gold wires (Goodfellow, Berwyn, PA) using a technique similar to that described in the literature [44]. The tip of a borosilicate capillary tube (2.0 mm o.d., 0.5 mm i.d.) was melted in a methane + air flame until the tip sealed. A 25 μm diameter gold electrode wire was inserted into the capillary tube and sealed in the glass by pulling a vacuum on the open end while simultaneously heating the sealed end of the glass with a coil of nichrome wire. Once several millimeters of the glass sealed around the wire, heating was stopped and electrical contact was made to the gold wire with a copper contact wire through the open end of the tube using either mercury or a silver epoxy (Epotek, Billerica, MA) and cured in an oven at 100°C for 1 h. The connecting wire was then fixed into place with Conap Easypoxy (Conap, Inc., Olean, NY) and cured at 100°C for a period of 4 h. Once sealed, the tip was shaped to achieve a conical geometry with emery paper (600 and 1200 grit). The exposed end was then polished to give a disk-in-plane geometry with a glass to metal ratio (R_g) greater than 10:1. Following initial shaping, the tip electrode was polished to a mirror finish using silica polish (1 and 0.05 μm), sonicated in an ethanol + water solution, and rinsed with de-ionized water before use.

Substrate electrodes consisted of 2 mm diameter commercial polycrystalline platinum disk electrodes (Bioanalytical Systems, West Lafayette, IN) encased in PEEK. Electrode pre-treatment consisted of polishing with successively finer grades of emery paper followed by diamond polishing paste until the electrodes exhibited a mirror finish. Before use, the substrate electrodes were sonicated in an ethanol + water solution and then rinsed with copious amounts of de-ionized water. Electrode pretreatment was achieved by electrochemical potential cycling between water oxidation and hydrogen evolution in an aqueous solution of 0.5 M H_2SO_4 until a characteristic voltammetric signature was obtained. Reference electrodes consisted of Ag | AgCl quasi-reference electrodes. The potential scale of these electrodes was verified against a standard calomel electrode and converted to the reversible hydrogen (RHE) scale. All data are presented versus the RHE electrode.

3. Results and discussion

The response of the tip electrode to potential cycling in a solution containing 0.01 M H_2SO_4 in argon saturated 0.1 M Na_2SO_4 is shown in Fig. 1a. The tip electrode, which is a 25 μm diameter gold microelectrode, exhibits minimal current at potentials positive of 0.0 V but an appreciable cathodic current at negative potentials corresponding to the reduction of protons (H^+) to hydrogen (H_2).

$$2H^+ + 2e^- \rightarrow H_2 \quad (1)$$

Although the formal potential of the hydrogen (H^+/H_2) couple resides at approximately 0.0 V on this potential scale (RHE), gold exhibits a large overpotential for the hydrogen evolution reaction [45]. Therefore, an appreciable reduction of H^+ is not observed until potentials negative of -0.5 V are reached. A steady, mass transfer-limited reduction current is achieved at potentials between -0.7 and -1.2 V. Bulk water reduction occurs at potentials negative of -1.2 V. A steady plateau current in the diffusion-limited region is maintained for this reaction under conditions where bubble formation does not occur, which is associated with the solubility limit of H_2 in this solution and typically requires hydrogen concentrations of less than 0.05 M. Further negative excursions in the tip potential (< -1.2 V) result in the reduction of bulk water and vigorous H_2 bubbling at the probe tip. The diffusion-limited current for hydrogen reduction under these conditions is approximately -340 nA.

With the microelectrode tip held at a potential of -1.0 V (denoted with * in Fig. 1a), the reduction of protons to hydrogen occurs at a diffusion-limited rate. Under these conditions, the SECM probe tip can perform a variety of functions when placed near a substrate interface. These functions include dosing of H_2 to

the substrate, detecting H^+ produced in the tip–substrate gap, and increasing the local solution pH. At small tip–substrate separations, H_2 that is generated at the tip diffuses to the substrate and is oxidized back to H^+, which can diffuse back to the tip and contribute to additional tip current. In this feedback mode, the tip current will reflect the rate of the hydrogen oxidation reaction at the substrate electrode and can be used to determine the value of the substrate rate constant for that reaction.

Fig. 1b illustrates the response of the platinum substrate electrode in the same electrolyte solution. The substrate is a 2 mm diameter platinum disk that exhibits behavior typical of polycrystalline Pt in sulfuric acid solution [46]. Peaks corresponding to hydrogen adsorption and desorption (H_{upd}) appear at potentials between 0.1 and 0.4 V. The more positive peaks at approximately 0.35 V are often attributed to strongly adsorbed hydrogen on Pt(100) regions. The more negative peaks at 0.2 V reflect less strongly bound hydrogen on Pt(110) surfaces. The broad background current between 0.1 and 0.4 V represents hydrogen adsorption onto Pt(111). The double layer region between 0.4 and 0.8 V on the positive scan is relatively featureless and reflects a clean metal surface, although bisulfate adsorption does occur in this region [7]. Hydroxide adsorption and then oxide formation occur at potentials near and above 0.8 V, while the onset of bulk water oxidation occurs at approximately 1.6 V. Oxide reduction appears in the negative scan with a peak centered at 0.75 V.

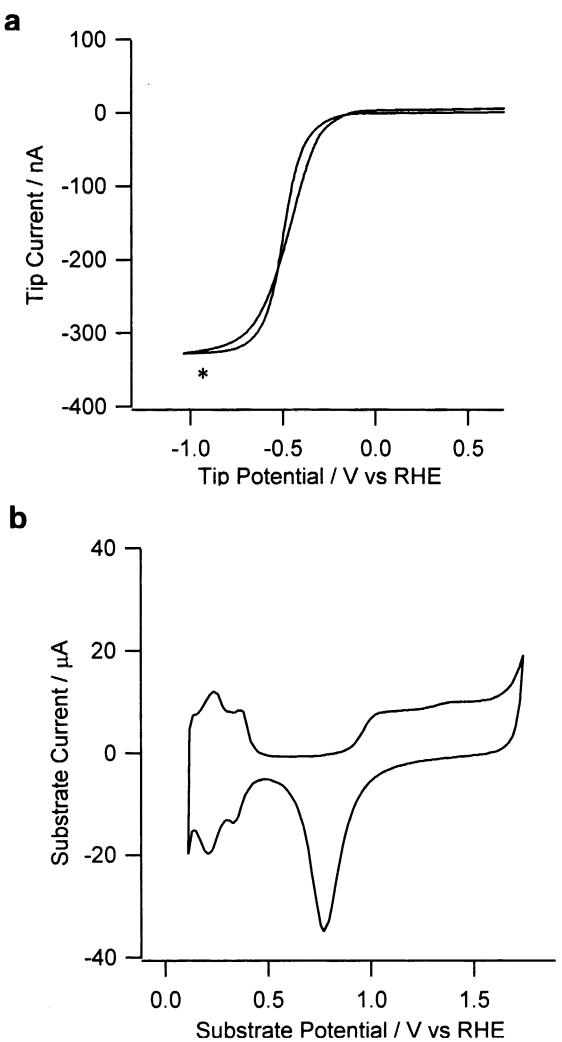

Fig. 1. (a) Cyclic voltammetry of a 25 μm diameter Au microelectrode in argon purged aqueous solution containing 0.01 M H_2SO_4 and 0.1 M Na_2SO_4 at a scan rate of 20 mV s^{-1}. The tip potential for subsequent measurements of the hydrogen oxidation reaction is denoted by *. (b) Cyclic voltammetry of a 2 mm diameter polycrystalline Pt electrode in argon purged 0.01 M H_2SO_4 and 0.1 M Na_2SO_4 at a scan rate of 200 mV s^{-1}.

A series of approach curves to this platinum substrate using a gold tip electrode are shown in Fig. 2a. The tip potential is held at -1.0 V, where the tip reaction is the diffusion-limited proton reduction (Eq. (1)). In these experiments, the tip is initially positioned at a relatively large separation from the substrate (~ 100 μm). The tip current is then monitored as the tip–substrate separation is decreased. Fig. 2a (open circles) illustrates the tip current (I_{tip}) normalized with respect to the current in the absence of the substrate ($I_{tip,\infty}$) as a function of the tip–substrate separation (d) normalized with respect to the tip radius ($a = 12.5$ μm). Approach curves acquired at substrate potentials ranging from 0.1 to 1.5 V are shown. At low substrate potentials, the approach curves exhibit positive feedback. This indicates a high rate of the back reaction ($k_{b,s}$), which is the hydrogen oxidation reaction, at the substrate electrode (Fig. 2a, inset left). Pure positive feedback is observed over a large potential range starting just above the reversible potential (> 0.1 V) and extending into the double layer region (< 0.7 V). At potentials where the platinum surface oxidizes (> 0.8 V), the degree of positive feedback decreases. At sufficiently positive potentials (> 1.3 V), the approach curve exhibits pure negative feedback corresponding to the presence of a non-reactive, platinum oxide covered surface (Fig. 2a, inset right).

The tip | substrate interface in the SECM system has been successfully modeled by considering the concentration of probe species, or in this case hydrogen generated and protons consumed at the tip electrode, by solution of the diffusion-reaction problem in cylindrical coordinates [47]. For hydrogen this problem is described by

$$\frac{\partial c_{H_2}}{\partial t} = D_{H_2}\left(\frac{\partial^2 c_{H_2}}{\partial z^2} + \frac{1}{r}\frac{\partial c_{H_2}}{\partial r} + \frac{\partial^2 c_{H_2}}{\partial r^2}\right) \quad (2)$$

and for protons is governed by

$$\frac{\partial c_{H^+}}{\partial t} = D_{H^+}\left(\frac{\partial^2 c_{H^+}}{\partial z^2} + \frac{1}{r}\frac{\partial c_{H^+}}{\partial r} + \frac{\partial^2 c_{H^+}}{\partial r^2}\right) \quad (3)$$

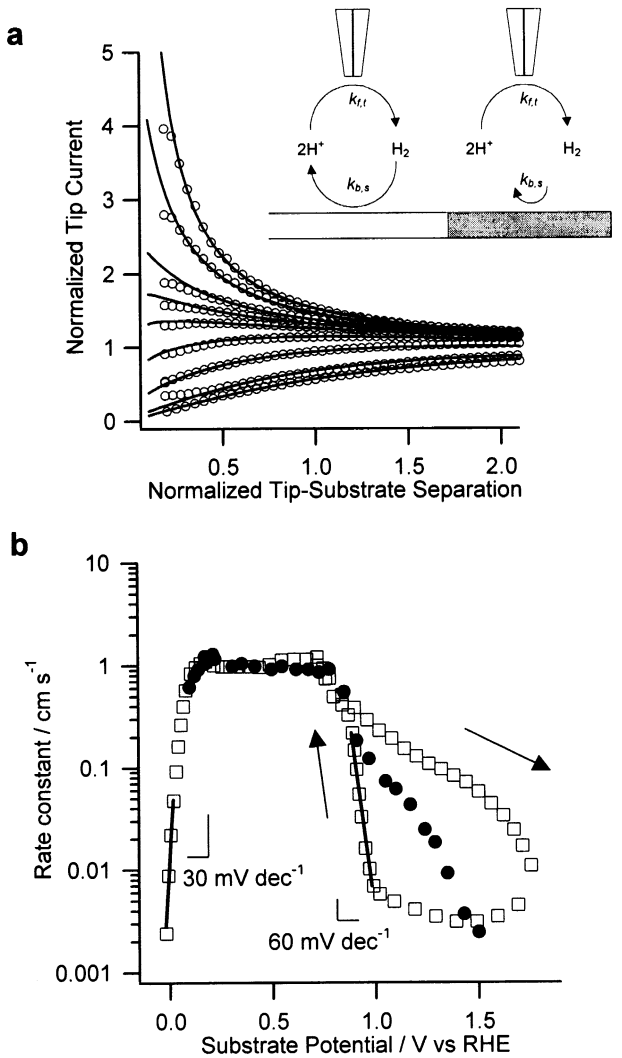

Fig. 2. (a) Experimental tip–substrate approach curves (open circles) at substrate potentials between 0.1 V (top curve) and 1.5 V (bottom curve) and tip potential of −1.0 V. Solid lines represent best fits of the theoretical feedback response as a function of the heterogeneous rate constant. Inset: schematic of the tip | substrate interface at low (left) and high (right) potentials. (b) Plot of the heterogeneous rate constant for H_2 oxidation on a polycrystalline platinum electrode as a function of applied potential in a solution containing 0.01 M H_2SO_4 and 0.1 M Na_2SO_4. Filled circles: fits from steady state approach curves with tip and substrate held at a constant potential. Open squares: fits from slow tip–substrate voltammetry at a separation of 4.25 μm and a scan rate of 2 mV s^{-1}. The arrows indicate the potential scan direction during the tip–substrate voltammetry.

Since the tip electrode is held at a potential where proton reduction is diffusion limited, the concentration of H^+ at the tip | electrolyte interface is zero and the H_2 concentration is determined by the rate of H^+ reduction.

The boundary condition at the substrate electrode is determined by the rate of hydrogen oxidation at that interface. If we consider a first order rate expression for the hydrogen oxidation reaction, the substrate boundary condition is

$$\frac{I}{nFA} = D\frac{dc_{H_2}}{dz} = k_{b,s}c_{H_2} \quad (4)$$

where $k_{b,s}$ is the rate constant for hydrogen oxidation in units of cm s^{-1}. The back reaction of H^+ reduction is assumed to occur at a negligible rate at the substrate electrode. A solution to Eqs. (2) and (3) under steady state conditions as a function of tip–substrate separation provides a series of working curves for the tip's current response [47–49]. These working curves can be fit to the experimentally measured tip current. Since the tip–substrate separation and tip radius are known, the only adjustable parameter in this model is the electrochemical rate constant $k_{b,s}$. This fitting procedure has been successfully applied in the measurement of rate constants for a variety of systems ranging from liquid | liquid interfaces to numerous heterogeneous electrochemical reactions [38,49].

The results from fitting the experimental approach curves are shown in Fig. 2a (solid lines). The rate constants extracted from these best-fit curves are summarized in Fig. 2b. Several different experiments are shown. Data from fitting steady state approach curves starting at low potentials and increasing to higher values are shown (Fig. 2b, filled circles). In addition, rate constants are shown that were extracted using the tip current response from tip–substrate voltammetry (TSV) (Fig. 2b, open squares). In these experiments, the tip–substrate separation was held fixed at 4.25 μm while the substrate potential was scanned at a rate of 2 mV s^{-1}. The forward and reverse scans are indicated by the arrows.

At low potential values near the reversible potential, the rate constant for the hydrogen oxidation reaction is low and increases in an exponential fashion with increasing substrate potentials. Fitting the low potential portion of this curve to a Tafel-like expression gives a slope of approximately 28 mV dec^{-1}, which is in close agreement with Tafel slopes of near 30 mV dec^{-1} as determined with rotating disk measurements. These results are consistent with the Tafel–Volmer mechanism where the dissociation of adsorbed hydrogen into surface adatoms is the rate determining step [2,5,7]. A line with Tafel slope of 30 mV dec^{-1} is shown on the plot for comparison. With increasing positive potentials, the rate constant continues to increase and then plateaus at a potential near 0.1 V. This reflects the transition to diffusion-limited conditions in the tip–substrate gap and corresponds to the upper limit of measurable rate constant values for this measurement. Rate constants as high as 10 cm s^{-1} for this reaction have been measured with 'better' tips that allow smaller tip–substrate gaps to be achieved [50]. In this case, diffusion-limited conditions, as indicated by pure positive feedback in the approach curves, are maintained until the potential exceeds 0.75 V. The formation of platinum oxide commences at approximately 0.75 V

and, correspondingly, the rate constant measured for hydrogen oxidation decreases.

The decrease in the hydrogen oxidation rate is strongly influenced by the oxide formation rate. This is illustrated by the three curves reflecting various rate constants in the oxide region between 0.8 and 1.7 V in Fig. 2b. Ultimately, the oxide coverage and thickness determine the catalytic activity towards the hydrogen oxidation reaction. The highest rate constants are observed in the oxide region for the tip–substrate voltammetry experiments during the forward moving potential scan (Fig. 2b, open squares and positive arrow). At these scan rates (2 mV s^{-1}), the oxide growth rate is slow such that the maximum oxide thickness is not obtained at a given potential. Thus, a higher rate constant is observed at each potential during the forward going scan. In contrast, during the steady-state approach experiments (Fig. 2b, closed circles), the substrate potential is held at a given potential for sufficient time for the oxide to grow completely and achieve its limiting thickness. Thus, the steady state approach curves reflect a lower rate constant, which is consistent with the maximum oxide thickness at a given potential. The lowest rate constants are observed for the reverse scan of the tip–substrate voltammetry (Fig. 2b, open squares and negative arrow). In this case, a thick oxide layer is present on the surface initially and remains until a potential is reached such that the oxide is removed from the surface. The rate constant remains low until the oxide is removed, whereby it quickly increases and reaches the diffusion limited value corresponding to the bare metal. The oxide reduction has a slope of approximately 60 mV dec^{-1} as shown in Fig. 2b. This is not a true Tafel slope for the hydrogen oxidation reaction but instead reflects the blocking effect of the platinum oxide and the kinetics of the oxide reduction process.

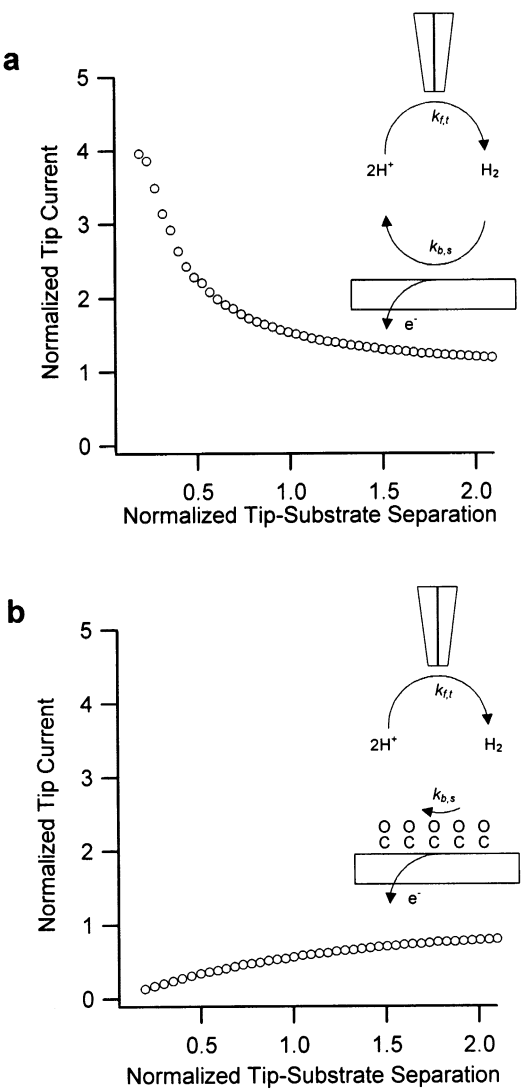

Fig. 3. Approach to a platinum electrode at open circuit in an argon-saturated solution containing 0.01 M H_2SO_4 and 0.1 M Na_2SO_4 with the tip electrode held at -1.0 V. (b) Approach to a platinum electrode at open circuit in a carbon monoxide-saturated solution containing 0.01 M H_2SO_4 and 0.1 M Na_2SO_4 with the tip held at -1.0 V. Inset: schematic of the tip | sample interface in argon and CO saturated solutions.

The hydrogen oxidation kinetics presented here are consistent with previous experiments using rotating disk measurements [2,5,7]. However, the SECM technique allows considerably higher rate constant values to be measured. In addition, the tip reaction can be selected to probe and isolate specific substrate processes, such as hydrogen oxidation in this case. In systems where multiple reactions can occur simultaneously on the substrate, the tip response can be used to deconvolute the substrate character for individual processes or reactions. In addition, the ability to scan the tip allows reactivity to be mapped over a heterogeneous surface [39,50], which allows structure–reactivity and catalyst screening experiments to be performed.

The oxidation of hydrogen in the presence of carbon monoxide is of significant practical consequence for fuel cells that operate using fuel derived from reformed hydrocarbons. Although CO adsorption on platinum has been extensively studied both with electrochemical and ultra-high vacuum methods, the potential-dependent kinetics and the dynamic effects of CO on hydrogen oxidation remain somewhat unclear [15,51]. In order to address the influence of CO adsorption on the hydrogen oxidation reaction, we conducted a series of SECM experiments in the presence of adsorbed CO using hydrogen reduction as the tip reaction. Fig. 3 depicts approach curves to a platinum substrate in the absence (Fig. 3a) and presence (Fig. 3b) of adsorbed CO. For both curves, the platinum electrode was placed in a solution containing 0.01 M $H_2SO_4 + 0.1$ M Na_2SO_4. The solution was purged with argon in the former and CO in the latter. To ensure complete adsorption of CO, the electrode was placed in a CO-saturated solution for a period of not less than 5 min before experiments were conducted. At open circuit, the bare

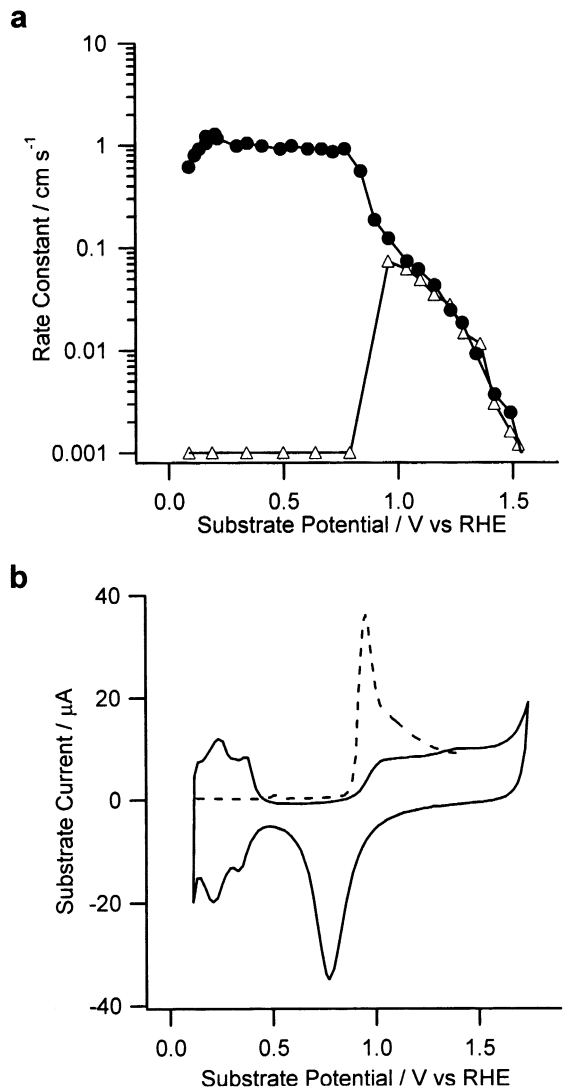

Fig. 4. Plot of heterogeneous rate constant values for H_2 oxidation at a platinum electrode in argon purged (filled circles) and carbon monoxide purged (open triangles) solution. These data were determined by fitting experimental steady state approach curves with the tip and substrate held at constant potential. (b) Plot of the voltammetric response of a platinum electrode in solution containing 0.01 M H_2SO_4 and 0.1 M Na_2SO_4 at a scan rate of 200 mV s^{-1}: (solid line) argon purged solution and (dashed line) carbon monoxide purged solution following CO adsorption at 0.0 V.

platinum electrode exhibits the expected positive feedback (Fig. 3a), which is indicative of a high substrate rate constant ($k_{b,s}$) for the hydrogen oxidation reaction. In contrast, adsorbed CO (Fig. 3b) exhibits pure negative feedback at open circuit, which indicates a rate constant below the measurable limit for this technique. In our hands, this lower limit is approximately 0.001 cm s^{-1}. This value is limited by the quality of the SECM tip and the sensitivity of the model to small rate constant values. Clearly, the adsorbed CO interferes with the hydrogen adsorption step and drastically reduces the rate of the oxidation reaction.

To explore more thoroughly the potential-dependence of the hydrogen oxidation reaction in the presence of CO, a series of approach curves was acquired. In each measurement, the platinum substrate was fully oxidized and then reduced to metal and held for a period of 5 min at different potentials between the limits of 0 and 1.6 V, in a CO saturated solution containing 0.01 M $H_2SO_4 + 0.1$ M Na_2SO_4. An approach curve was then conducted starting at a tip–substrate separation of 100 μm. At each substrate potential, a steady-state approach curve consisting of the normalized tip current as a function of normalized tip–substrate separation was fit to a theoretical working curve in order to determine the hydrogen oxidation rate constant. Fig. 4a depicts the rate constants determined for the hydrogen oxidation reaction in the presence of adsorbed CO (open triangles). Results in the absence of adsorbed CO from steady state approach curves are included for comparison (Fig. 4a, filled circles).

In the presence of adsorbed CO, the rate constant value for hydrogen oxidation is near zero for potentials less than 0.8 V. In this potential regime, pure negative feedback was observed, indicating that the reaction rate was below the measurable limit for the SECM technique (~ 0.001 cm s^{-1}). Although the CO coverage decreases as the adsorption potential becomes more positive [51], we see that the CO adlayer poisons the platinum substrate towards hydrogen oxidation over this entire potential range. The rate constant increases to a measurable value as the potential exceeds 0.8 V. Above this potential, the carbon monoxide no longer adsorbs on the surface but water adsorbs to form platinum oxides according to

$$Pt + xH_2O \rightarrow PtO_x + 2xH^+ + 2xe^- \quad (5)$$

In the absence of the CO layer, the hydrogen oxidation rate constant achieves a level consistent with the platinum oxide and decreases accordingly with increasing potential as the oxide layer thickens. The substrate CV in the presence of dissolved CO (Fig. 4b, dashed line) exhibits enhanced current in the oxide region due to the oxidation of CO from solution.

The steady state response of CO-covered platinum, as deduced by approach curve measurements, indicates that the surface is completely poisoned to the hydrogen oxidation reaction at potentials below platinum oxide formation. In order to examine the dynamics involved with CO oxidation and its influence on the hydrogen oxidation reaction, tip–substrate voltammetry (TSV) experiments were performed in CO-containing solutions. Fig. 5 depicts two sets of TSV experiments corresponding to two different CO adsorption potentials. Prior to each experiment, the platinum substrate was oxidized thoroughly and then reduced to metal and held at a fixed potential in a CO saturated solution

containing 0.01 M $H_2SO_4 + 0.1$ M Na_2SO_4 in order to adsorb CO. After CO was adsorbed, the substrate potential was scanned in the positive direction starting at the adsorption potential and moving positive at a rate of 20 mV s^{-1}. Fig. 5a (dashed line) shows the substrate response following CO adsorption in the hydrogen adsorption region (H_{upd}) at 0.1 V. The base substrate response for CO desorption is characterized by a pre-oxidation wave in the region between 0.3 and 0.8 V followed by a main oxidation wave at 0.9 V. The pre-oxidation wave has been attributed to the oxidation of weakly adsorbed CO ($CO_{ads,w}$) by adsorbed hydroxide (OH_{ads}) or water molecules [51]. This weakly adsorbed adlayer is formed following CO adsorption in the upd-H region. The presence of surface OH or water molecules is sufficient to oxidize a portion of this weakly adsorbed CO layer [51]. Following partial CO oxidation, the remaining CO on the surface rearranges to form a more strongly bound CO layer with a different surface structure. The main oxidation peak centered at 0.9 V is associated with electro-oxidation of this strongly bound CO layer to carbon dioxide, which presumably is nucleated by hydroxide or oxide formation on the platinum substrate. In the presence of CO in solution, the main CO oxidation wave shifts 0.2 to 0.3 V positive of the oxidation peak in CO-free solution, which is typically near 0.8 V (RHE). This increase in potential is due to a competition for surface sites between OH and CO from solution [52].

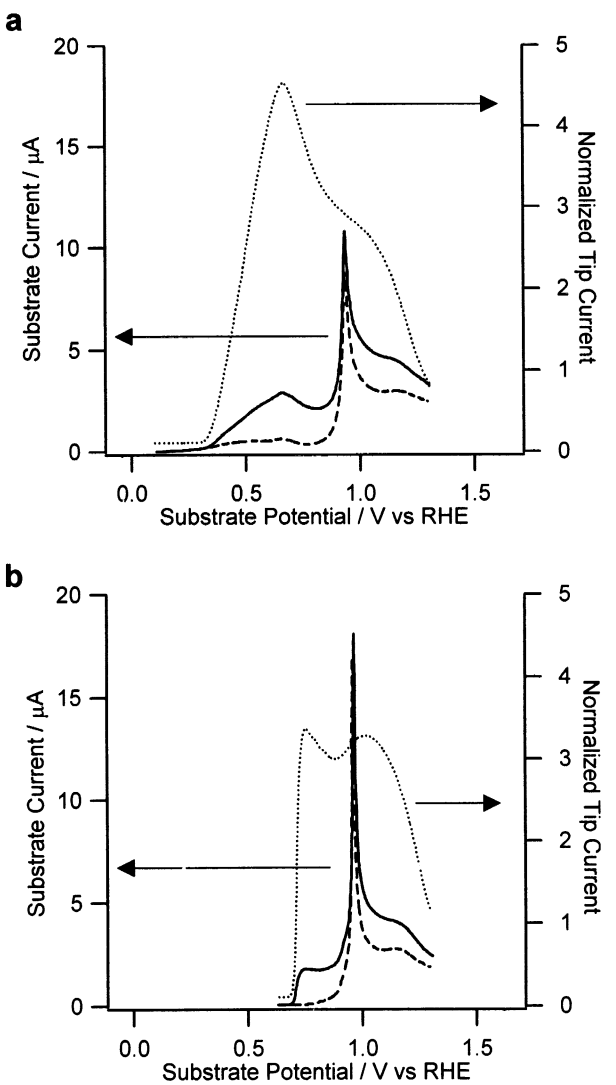

Fig. 5. Tip–substrate voltammetry of a platinum substrate electrode in a carbon monoxide-saturated solution containing 0.01 M H_2SO_4 and 0.1 M Na_2SO_4 in the absence (dashed line) and presence (solid line) of the SECM tip at a substrate scan rate of 20 mV s^{-1}. The SECM tip is held at a potential of -1.0 V where the reduction of protons occurs at a diffusion-limited rate. The tip response (dotted line) corresponds to a tip–sample separation of 1 μm. (a) CO adsorption potential of 0.1 V. (b) CO adsorption potential of 0.6 V.

The influence of the adsorbed CO layer on the hydrogen oxidation reaction can be deduced by placing the microelectrode tip at a separation of approximately 1 μm from the substrate. Fig. 5a illustrates the tip (dotted line) and substrate (solid line) current response to changes in the substrate potential after CO was pre-adsorbed on the substrate at 0.1 V. The tip current at potentials below 0.3 V is near zero, which reflects negative feedback between the tip and the CO-covered substrate due to a low hydrogen oxidation rate. At these potentials, the adsorbed CO layer completely blocks the substrate for the hydrogen oxidation reaction. As the substrate potential is increased to values above 0.3 V, the tip current increases and reaches a local maximum at 0.7 V. This increase in the tip current is primarily the result of positive feedback between the tip and substrate, which results from an increase in the rate of hydrogen oxidation at the substrate electrode. An increase in the substrate current is also observed in this potential range in the presence of the tip. This is due to hydrogen oxidation at the substrate electrode, which occurs because of H_2 dosed to the substrate via the tip. The increase in the tip and substrate current coincides with the appearance of the pre-oxidation wave at the substrate voltammogram observed in the absence of the tip (Fig. 5a, dashed line), indicating that oxidation of the weakly adsorbed CO in this region has resulted in the appearance of reaction sites capable of oxidizing hydrogen.

Hydrogen oxidation in this low potential region can be considered to be occurring through a CO-covered surface. The weakly bound CO layer that forms at low potentials converts into a strongly bound layer following oxidation of a portion of the CO adlayer. Although steady state approach curves show that the platinum surface is covered with CO and inactive towards hydrogen oxidation over this entire potential range, transient reaction sites form in the CO layer during the potential-induced conversion between these adsorbed forms. The

number of reaction sites is sufficient to allow a considerable increase in the hydrogen oxidation rate. In fact, the maximum current attained during this positive scan corresponds to diffusion-limited conditions between tip and substrate, which gives a rate constant in excess of 1 cm s^{-1}. However, if the substrate potential is held at any value in this transition region in the presence of solution CO, the enhanced current at the tip and substrate decays over a period of several minutes until a completely blocking CO layer reforms on the surface, which is consistent with the steady state approach curve results. The subsequent decrease in the tip current in Fig. 5a is due to the re-poisoning of the substrate by the remaining CO molecules on the substrate and/or by adsorption from solution. As the substrate potential exceeds 0.8 V, the tip current responds to the oxidation of strongly bound CO. The tip current increases slightly as the CO layer is oxidatively desorbed and then decreases again as the platinum oxide is formed. This behavior is consistent with the hydrogen oxidation rate observed in Fig. 4a at potentials where CO is not adsorbed and the platinum oxide forms. Increasing the substrate potential to higher potentials leads to increasingly negative feedback as a result of the platinum oxide growth.

The nature of the adlayer CO coverage on platinum changes with increasing substrate adsorption potential. At sufficiently positive adsorption potentials, the weakly adsorbed CO layer does not form and the pre-oxidation wave is absent [15,51]. Instead, the strongly bound CO layer forms directly via adsorption onto the surface. This case is observed in Fig. 5b, where CO was pre-adsorbed at a potential of 0.6 V, which is in the double layer region. As opposed to Fig. 5a, only the main CO oxidation peak is observed in the substrate current response (Fig. 5b, dashed line). The absence of the weakly bound CO layer leads to the absence of the pre-oxidation wave and CO oxidation is inhibited until the main peak is observed at approximately 0.9 V.

The influence of this CO adlayer on the hydrogen oxidation reaction can again be examined by placing the SECM tip electrode near (~ 1 μm) the substrate and performing tip–substrate voltammetry (TSV). Fig. 5b illustrates the tip (dotted line) and substrate (solid line) current response to changes in the substrate potential after CO is pre-adsorbed at a potential of 0.6 V. At potentials closest to the adsorption potential, negative feedback is observed. This is followed by an increase in both the tip and substrate current prior to the appearance of the main oxidation wave at a potential of approximately 0.8 V. Positive feedback at the tip implies that the hydrogen oxidation reaction is taking place at the substrate in this potential region below the main CO oxidation wave.

The most likely explanation for this enhanced hydrogen oxidation current involves the formation of reactive surface sites due to the presence of the tip. Steady state tip–sample approach curves (Fig. 4a) indicate that the rate constant for hydrogen oxidation remains near zero until the platinum oxide forms, which is the potential where the main CO oxidation occurs. However, results presented in Fig. 5a suggest that the oxidation of a small quantity of CO is sufficient to create a surface that is highly active for the hydrogen oxidation reaction. Thus, the low potential oxidation of hydrogen at 0.8 V in Fig. 5b, which is more than 0.2 V below the main CO oxidation wave, must clearly be the result of a restructuring of the CO adlayer due to a structural transformation or partial oxidation/desorption of CO. Either process could be driven by a local increase in solution pH via proton reduction at the tip. Since the tip is depleting protons in the tip–substrate gap, the nucleation of OH on the platinum substrate may be enhanced. Competitive binding of OH with CO could drive a structural transformation in the CO adlayer such that active sites emerge on the platinum surface. Alternatively, the tip could be driving CO off the surface at lower potentials via oxidative desorption according to the reaction described in Eq. (6).

$$CO_{ads} + OH_{ads} \rightarrow CO_2 + H^+ + e^- \quad (6)$$

The depletion of H^+ drives this reaction in the forward direction thereby increasing the rate of oxidation of the adsorbed CO. Ultimately, the oxidative desorption seems less likely because the magnitude of the main CO oxidation peak, which is proportional to the CO coverage, is comparable with and without the tip near the substrate. Notably, an increase in pH has been shown to lower significantly the potential for CO oxidation on Pt surfaces [53]. A final possibility would be that a structural transformation is occurring in the adlayer due to the applied potential that is providing reactive sites for CO oxidation. We are currently attempting to verify the origin of this effect.

Further positive excursions in the substrate potential lead to a drop in the tip current. The drop in current at 0.9 V must be due to a reduction in the available hydrogen adsorption sites, which is probably due to the emergence of the platinum oxide. Subsequently, the main CO oxidation peak is observed and the tip current increases as the CO layer is removed from the surface. Increasingly positive substrate potentials lead to growth of the platinum oxide and a decrease in the hydrogen oxidation rate as illustrated by a drop in the tip current due to negative feedback.

4. Conclusions

We have described an application of the scanning electrochemical microscope that characterizes the kinetics of the hydrogen oxidation reaction on platinum. As a tool for measuring electrochemical reaction kinetics, SECM has some benefit over more traditional hydrodynamic methods. In particular, rate constant values in excess of those readily measured with rotating disk techniques are accessible with SECM. In this work, the hydrogen oxidation rate was measured over four orders of magnitude with little difficulty. The Tafel slope of 28 mV dec^{-1} for polycrystalline platinum is consistent with published results. One of the more significant advantages of SECM is the ability to probe a specific reaction or process and use that information to decouple the response of a substrate electrode. This is particularly useful in complex or multi-step processes where the current measured at a working electrode has contributions from multiple sources. This capability was utilized here to deduce the influence of adsorbed CO and oxide formation on the hydrogen oxidation reaction on platinum. As expected, the steady-state response of adsorbed CO was to deactivate platinum completely towards hydrogen oxidation. However, the enhancement of hydrogen oxidation as seen with tip–substrate voltammetry (TSV) in the double layer region during the transformation between weakly and strongly bound CO adlayers suggests that very small variations in the adlayer structure are needed to sustain appreciable rates of the hydrogen oxidation reaction. We are currently exploring the dynamics and temperature dependence of this transition region on pure platinum and platinum alloy surfaces as well as developing the imaging capabilities of this method for catalyst screening experiments.

Acknowledgements

ACH would like to acknowledge the Office of Naval Research for a Young Investigator Award, the Camille and Henry Dreyfus Foundation for a New Faculty Award, and the Donors of The Petroleum Research Fund as administered by the American Chemical Society, for partial support of this research. ACH also wishes to thank Molecular Imaging Corporation for a Young Electrochemical Scanning Probe Microscopist Award. JLH would like to acknowledge the National Science Foundation for partial support of this research.

References

[1] K.J. Vetter, Electrochemical Kinetics, Academic Press, New York 1967.
[2] A. Frumkin, V. Sobol, A. Dmitrieva, J. Electroanal. Chem. 13 (1967) 179.
[3] S. Schuldiner, J. Electrochem. Soc. (1968) 362.
[4] S. Schuldiner, M. Rosen, D.R. Flinn, J. Electrochem. Soc. 117 (1970) 1251.
[5] L.I. Krishtalik, in: P. Delahay, C.W. Tobias (Eds.), Advances in Electrochemistry and Electrochemical Engineering, vol. 7, Wiley, New York, 1970.
[6] S. Trasatti, in: H. Gerisher, C.W. Tobias (Eds.), Advances in Electrochemistry and Electrochemical Engineering, vol. 10, Wiley, New York, 1977.
[7] N.M. Markovic, B.N. Grgur, P.N. Ross, J. Phys. Chem. B 101 (1997) 5405.
[8] P.N. Ross, in: P.N. Ross, J. Lipkowski (Eds.), Electrocatalysts, Wiley, New York, 1998, p. 1.
[9] E. Herrero, J. Clavilier, J.M. Feliu, A. Aldaz, J. Electroanal. Chem. 410 (1996) 125.
[10] M.W. Breiter, J. Electroanal. Chem. 65 (1975) 623.
[11] H.A. Gasteiger, N.M. Markovic, P.N. Ross, J. Phys. Chem. 99 (1995) 16757.
[12] H. Igarashi, T. Fujino, M. Watanabe, J. Electroanal. Chem. 391 (1995) 119.
[13] C. McCallum, D. Pletcher, J. Electroanal. Chem. 70 (1976) 277.
[14] L. Grambow, S. Bruckenstein, Electrochim. Acta 22 (1977) 377.
[15] H. Kita, H. Naohara, T. Nakato, S. Taguchi, A. Aramata, J. Electroanal. Chem. 386 (1995) 197.
[16] N.M. Markovic, C.A. Lucas, B.N. Grgur, P.N. Ross, J. Phys. Chem. B 103 (1999) 9616.
[17] S.J. Lee, S. Mukerjee, E.A. Ticianelli, J. McBreen, Electrochim. Acta 44 (1999) 3283.
[18] Kitamura, M. Takahashi, M. Ito, Surf. Sci. 223 (1989) 493.
[19] B. Beden, A. Bewick, C. Lamy, J. Electroanal. Chem. 148 (1983) 147.
[20] S.-C. Chang, M.J. Weaver, J. Phys. Chem. 95 (1991) 5391.
[21] C. Korzeniewski, Crit. Rev. Anal. Chem. 27 (1997) 81.
[22] S. Baldelli, N. Markovic, P. Ross, Y.-R. Shen, G. Somorjai, J. Phys. Chem. B 103 (1999) 8920.
[23] K. Sashikata, N. Furuya, K. Itaya, J. Electroanal. Chem. 316 (1991) 361.
[24] I. Villegas, M.J. Weaver, J. Chem. Phys. 101 (1994).
[25] K.A. Freidrich, K.-P. Geyzers, U. Linke, U. Stimming, J. Stumper, J. Electroanal. Chem. 402 (1996) 123.
[26] H.A. Gasteiger, N. Markovic, P.N. Ross, E.J. Cairns, J. Phys. Chem. 98 (1994) 617.
[27] H.A. Gasteiger, N.M. Markovic, J.P.N. Ross, J. Phys. Chem. 99 (1995) 8290.
[28] R. Ianniello, V.M. Schmidt, U. Stimming, J. Stumper, A. Wallau, Electrochim. Acta 39 (1994) 1863.
[29] W.F. Lin, M.S. Zei, M. Eiswirth, G. Ertl, T. Iwasita, W. Vielstich, J. Phys. Chem. B 103 (1999) 6968.
[30] T.J. Schmidt, M. Noeske, H.A. Gasteiger, R.J. Behm, Langmuir 13 (1997) 2591.
[31] H.A. Gasteiger, N.M. Markovic, J.P.N. Ross, J. Phys. Chem. 99 (1995) 8945.
[32] H.A. Gasteiger, N.M. Markovic, P.N. Ross, Catal. Lett. 36 (1996) 1.
[33] B.N. Grgur, G. Zhuang, N.M. Markovic, P.N. Ross, J. Phys. Chem. B 101 (1997) 3910.
[34] B.N. Grgur, N.M. Markovic, P.N. Ross, J. Phys. Chem. B 102 (1998) 2494.
[35] B.N. Grgur, N.M. Markovic, P.N. Ross, J. Electrochem. Soc. 146 (1999) 1613.
[36] D.O. Wipf, A.C. Michael, R.M. Wightman, J. Electroanal. Chem. 269 (1989) 15.
[37] J.V. Macpherson, S. Marcar, P.R. Unwin, Anal. Chem. 66 (1994) 2175.

[38] M.V. Mirkin, L.O.S. Bulhoes, A.J. Bard, J. Am. Chem. Soc. 115 (1993) 201.
[39] B.C. Shah, A.C. Hillier, J. Electrochem. Soc. 147 (2000) 3043.
[40] J. Kwak, A.J. Bard, Anal. Chem. 61 (1989) 1794.
[41] A.J. Bard, F.-R.F. Fan, D.T. Pierce, P.R. Unwin, D.O. Wipf, F. Zhou, Science 254 (1991) 68.
[42] M.V. Mirkin, Anal. Chem. A 68 (1996) 177.
[43] A.J. Bard, D.E. Cliffel, C. Demaille, F.R.F. Fan, M. Tsionsky, Ann. Chim. 87 (1997) 15.
[44] C. Lee, C.J. Miller, A.J. Bard, Anal. Chem. 63 (1991) 78.
[45] J.O'M. Bockris, S.U.M. Khan, Surface Electrochemistry: A Molecular Level Approach, Plenum, New York, 1993.
[46] P.A. Christensen, A. Hamnett, Techniques and Mechanisms in Electrochemistry, Blackie, London, 1994.
[47] A.J. Bard, M.V. Mirkin, P.R. Unwin, D.O. Wipf, J. Phys. Chem. 96 (1992) 1861.
[48] D.O. Wipf, A.J. Bard, J. Electrochem. Soc. 138 (1991) 469.
[49] C. Wei, M.V. Mirkin, A.J. Bard, J. Phys. Chem. 99 (1995) 16033.
[50] B.C. Shah, K. Jambunathan, A.C. Hillier Localized In-Situ Methods for Investigating Electrochemical Interfaces, Honolulu, HA, 1999, pp. 175.
[51] N.M. Markovic, B.N. Grgur, C.A. Lucas, P.N. Ross, J. Phys. Chem. B 103 (1999) 487.
[52] A. Couto, M.C. Perez, A. Rincon, C. Gutierrez, J. Phys. Chem. 100 (1996) 19538.
[53] N.M. Markovic, T.J. Schmidt, B.N. Grgur, H.A. Gasteiger, R.J. Behm, P.N. Ross, J. Phys. Chem. B 103 (1999) 8568.